Educational Experimental Platform for Emulation of Photovoltaic Modules

Srđan Lale[1], Milomir Šoja[1], Slobodan Lubura[1] and Marko Ikić[1]

[1] Faculty of Electrical Engineering, University of East Sarajevo, East Sarajevo, Bosnia and Herzegovina

srdjan.lale@etf.ues.rs.ba, milomir.soja@etf.ues.rs.ba, slobodan.lubura@etf.ues.rs.ba, marko.ikic@etf.ues.rs.ba

Abstract—**This paper presents a one solution for photovoltaic (PV) emulator. A main part of the developed PV emulator is buck converter with recently proposed new I^2 dual current mode control (I^2 DCMC). The given simulation and experimental results demonstrate excellent performances of the proposed PV emulator: matching between the characteristics obtained from the developed mathematical (simulation) model of the PV module and from the PV emulator, adaptability to the emulated changes in solar insolation and temperature, simple and efficient manipulation with PV module parameters and operating conditions, which is useful especially for education purposes, and fast dynamics.**

Keywords-PV emulator; PV characteristics; buck converter; I^2 dual current mode control

I. INTRODUCTION

Photovoltaic (PV) modules have important role in renewable power sources today. However, there are some issues which make difficult the entire process of laboratory development and testing of existing and new PV applications: high cost of PV modules, dependence on weather conditions (solar insolation and temperature), etc. Therefore, the usage of output of real PV modules, which are installed outdoor, in laboratories is not so convenient, considering their high price and impossibility of controlling the testing conditions, because the PV module characteristics vary during the day with different levels of solar insolation and temperature. As an alternative, a device which emulates (simulates) the current-voltage (I-V) characteristic of real PV module – PV emulator, can be used instead, as power source for any PV system which is tested in laboratory environment.

Commercial PV emulators, e.g. [1], [2], are unfortunately very expensive and hard to be purchased. For that reason, there are many research activities dealing with development of low-cost PV emulators which can be used for education purposes and for prototyping of different PV systems. For example, in [3], [4], simple low-cost PV emulators are proposed, which are based on simple electronics designs, without power electronics converters. However, these emulators have low power ratings and not so high precision. Most of the PV emulators known in literature are based on DC-DC power electronics converters, especially on buck converter [5]-[13]. Although their complexity is increased, they offer higher power ratings, typical for PV modules and arrays, and much better matching between the characteristics of real and emulated PV modules.

In general case, the output of the DC-DC converter should behave as the output of the PV module, i.e. the converter's load voltage and current should mimic PV voltage and PV current. The buck converter is the most appropriate for the design of the PV emulator, because its output (load) current is equal to the average inductor current. Therefore, by controlling the average value of the inductor current of the buck converter, the load current could be directly controlled.

Different control concepts could be applied for the design of the PV emulator. For example, voltage mode control (VMC) of the buck converter-based PV emulator is proposed in [12]. The load current is measured and entered the mathematical model of the PV module. The model's output is reference PV voltage, which is used as a voltage reference for the output voltage regulator. However, considering that the PV modules are current sources by their nature, it is better using current mode control (CMC), especially having in mind all the benefits of CMC over VMC. Majority of the mentioned PV emulators employ CMC [5]-[11]. Usually, the load voltage is measured and fed into the PV model. The PV model calculates the reference PV current, which is used as a current reference for controlling the load current. There is also a possibility for combination of CMC and VMC, as it is suggested in [13], depending on the regions on the PV I-V curve.

Commonly, the calculated PV reference current is used as a reference current for the load current linear regulator, such as proportional-integral (PI) or proportional-integral-derivative (PID) regulator [6], [8], [10], [11]. In [7] and [9] the duty cycle is iteratively updated until the measured load current is equal to the calculated PV reference current.

Considering that the load current of the buck converter is equal to the average inductor current, the calculated PV reference current can be used as a reference inductor current, as it is proposed in [5], which means that the average current mode control (ACMC) can be applied. Also, in [11] is shown

that both current regulators can be used at the same time: the outer load current PI regulator and the inner inductor current regulator, which is based on predictive ACMC. Using this double CMC is not so necessary for the buck converter, however, when other type of the converter is used in the PV emulator, e.g. buck-boost, it is mandatory to use outer load current regulator, because the load current is not equal to the average inductor current. In that case, the outer load current regulator produces the reference current, which is used in the inner current loop for controlling the inductor current.

Important issue in practical realization of the PV emulator is implementation of the PV mathematical nonlinear model. The PV model could be implemented on various digitals platforms, such as microcontrollers or digital signal processors [5], [7], [8], [11], [13], field programmable gate arrays [9], [14], etc. Especially interesting is using Matlab/Simulink environment for real time implementation of the PV emulators, by utilization of data acquisition boards [12], [15], [16]. Real time interaction with Matlab/Simulink provides rapid prototyping and it is also very useful in education.

In this paper, the PV emulator based on buck converter with recently developed I^2 dual current mode control (I^2 DCMC) [17], is proposed. The PV model is implemented and executed in Simulink in real time, by using MF 624 data acquisition board, installed in PC computer. The calculated PV reference current is exported from the acquisition board and entered the developed control electronic module, which is based on I^2 DCMC. The I^2 DCMC ensures the equality between the PV reference current and the average inductor current. In this way, the load current is precisely matched with the PV reference current obtained from the PV model, regardless of the emulated weather conditions, such as different levels of solar insolation and temperature. Thanks to the excellent dynamical features of I^2 DCMC, the proposed PV emulator provides fast and precise tracking of different PV reference currents during the emulated changes in solar insolation, temperature and load.

This paper is organized as follows. Section II presents a description of the proposed PV emulator. Simulation and experimental results are given in Section III and Section IV, respectively. Concluding remarks are given in Section V.

II. DESCRIPTION OF THE PROPOSED PV EMULATOR

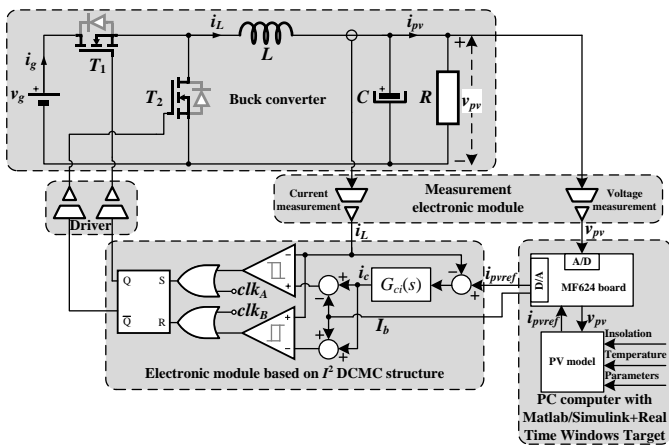The proposed PV emulator's structure is shown on Fig. 1.

Figure 1.   The structure of the proposed PV emulator.

A.   PV Model

The mathematical model of the PV module is derived from well-known single-diode equivalent circuit of the PV cell, with parallel and series resistances, which is shown on Fig. 2.
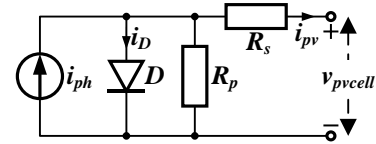

Figure 2.   Single-diode equivalent circuit of the PV cell.

The circuit from Fig. 2 can be described with following equations, which are given in [5]:

$$i_{pv} = i_{ph} - I_r \left(e^{\frac{q\left(v_{pvcell} + R_s i_{pv}\right)}{\eta k T}} - 1 \right) - \frac{\left(v_{pvcell} + R_s i_{pv}\right)}{R_p} \tag{1}$$

$$i_{ph} = \left[I_{sc} + \alpha \left(T - T_0 \right) \right] \frac{I_{ins}}{1000} \tag{2}$$

$$I_r = I_0 \left(\frac{T}{T_0} \right)^3 e^{\frac{q E_g \left(\frac{1}{T_0} - \frac{1}{T} \right)}{\eta k}} \tag{3}$$

$$I_0 = \frac{I_{sc} - \frac{V_{occell}}{R_p}}{e^{\frac{q V_{occell}}{\eta k T_0}} - 1} \tag{4}$$

$$v_{pvcell} = \frac{v_{pv}}{N_s}, \quad V_{occell} = \frac{V_{oc}}{N_s}, \tag{5}$$

where v_{pv} and i_{pv} denote voltage and current of the PV module, respectively, v_{pvcell} is the PV cell voltage, i_{ph} is photocurrent, I_{sc} is short-circuit PV current under standard test conditions (STC) – insolation 1000 W/m² and temperature 25°C (298 K), V_{oc} and V_{occell} are open-circuit voltages of the PV module and the PV cell, respectively, in STC, R_p and R_s are parallel and series resistances, I_r is diode reverse saturation current, I_0 is diode reverse saturation current in STC, I_{ins} is intensity of solar insolation, T is ambient temperature, T_0 is temperature in STC (T_0=298 K), α is temperature coefficient (α=6 mA/°C), q is electron charge (q=1.6×10⁻¹⁹ C), η is ideality factor of the p–n junction (η=1.01), k is Boltzmann constant (k=1.38×10⁻²³ J/K), E_g is band gap energy (E_g=1.1 eV) and N_s is number of series connected PV cells.

It is obvious from (1)-(5) that the PV model has three inputs: PV voltage v_{pv}, solar insolation I_{ins} and ambient temperature T, and one output: PV current i_{pv} from (1). The model parameters, such as I_{sc}, V_{oc} and other, are the standard PV module data-sheet parameters.

B.   Buck Converter

A main part of the proposed PV emulator is the synchronous buck converter (Fig. 1). The output of the buck converter represents the output of the emulated PV module: the load voltage and current mimic the PV voltage v_{pv} and the PV current i_{pv}, respectively. The input voltage v_g must be greater than the open-circuit voltage V_{oc} of the PV module. Therefore, the output voltage of the buck converter, i.e. the output voltage

of the PV emulator v_{pv} can range from zero to V_{oc}, depending on the working point on the PV emulator's I-V characteristic. The working point of the PV emulator is obtained as intersection between the load working line $i_{pv}=v_{pv}/R$, where R is the load resistance, and the PV I-V characteristic.

C. I^2 DCMC Structure

The I^2 DCMC, which is proposed in [17], is a novel CMC method, that provides the equality between the average value of the inductor current and the reference current, by using the inner current regulator $G_{ci}(s)$ (Fig. 1). The inductor current i_L is limited between upper i_c+I_b and lower i_c-I_b boundary, where i_c represents the output of the regulator $G_{ci}(s)$. The current bandwidth $2I_b$, i.e. the difference between the current limits, has predefined and constant value, and must be equal or greater than the maximum peak-to-peak ripple of the inductor current. By comparison of the inductor current i_L with the current limits $i_c\pm I_b$, the turning on/off instants of the power switches T_1 and T_2 are determined.

The load voltage of the buck converter v_{pv} is measured and used as the input of the PV model. The calculated PV current (1) is exported from the PV model and used as the reference current i_{pvref} for the regulator $G_{ci}(s)$ (Fig. 1). The regulator $G_{ci}(s)$ produces a necessary value of the control signal i_c to equalize the average inductor current $\langle i_L(t)\rangle_{T_s}$ over each switching period T_s with the PV reference current i_{pvref}:

$$\langle i_L(t)\rangle_{T_s} = i_{pvref} = i_{pv}. \qquad (6)$$

In this way, the load current i_{pv} is equal to the PV reference current i_{pvref} from (1).

The inner current regulator $G_{ci}(s)$ is implemented as a simple integral (I) regulator:

$$G_{ci}(s) = \frac{K_i}{s}. \qquad (7)$$

The procedure for the design of the regulator $G_{ci}(s)$ is presented in [17].

III. SIMULATION RESULTS

The parameters values which are used in simulations are listed in Table I. A generic PV module is considered, not some specific manufacture type. The simulations were performed in Simulink, for several case studies.

A. Stationary States for Different Values of Insolation and Temperature

First, the performances of the proposed PV emulator were tested in stationary state, for different levels of solar insolation and temperature. The simulation results are given in Fig. 3.

It is obvious from Fig. 3 that the obtained working points of the PV emulator – the output voltage v_{pv} and the output current i_{pv}, are matched perfectly with the expected working points – intersections between the load working line and the I-V curves of the PV model, for all considered insolations and temperatures.

TABLE I.   PARAMETERS OF THE PV EMULATOR

| Parameter	Description	Value
Buck converter		
v_g	Input voltage	28 V
L	Inductance	220 µH
C	Capacitance	1000 µF
R	Load resistance	4 Ω
I^2 DCMC		
f_s	Switching frequency	23 kHz
I_b	Half of the current bandwidth	0.8 A
K_i	Integral gain	5000
PV model		
I_{sc}	Short-circuit PV current in STC	3.8 A
V_{oc}	Open-circuit PV voltage in STC	21.1 V
V_{mpp}	Voltage at maximum power point (MPP) of PV module in STC	17.1 V
I_{mpp}	Current at MPP of PV module in STC	3.5 A
N_s	Number of series connected PV cells	36
R_s	Series resistance of PV cell	0.0102 Ω
R_p	Parallel resistance of PV cell	5.2022 Ω
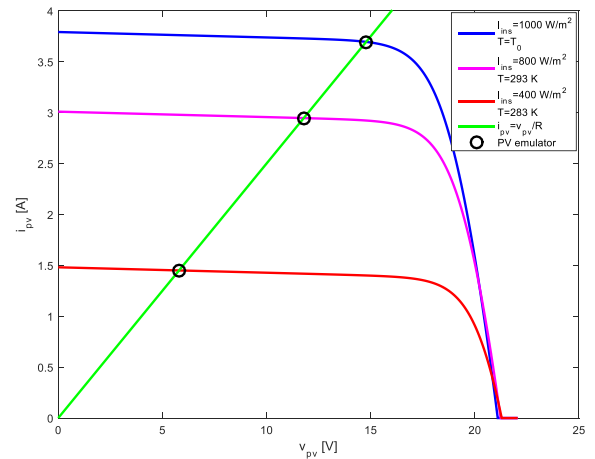
Figure 3.   Working points (round black markers) of the PV emulator and I-V curves of the PV model, for different solar insolations and temperatures: (1000 W/m², 298 K), (800 W/m², 293 K) and (400 W/m², 283 K).

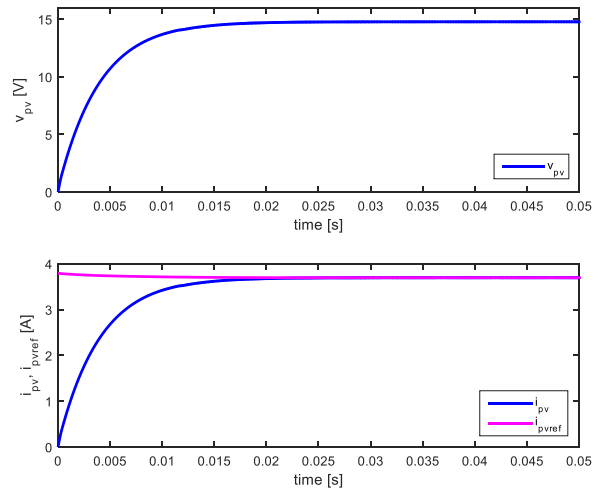Figure 4.   The output voltage and current of the PV emulator, for solar insolation 1000 W/m² and temperature 298 K (STC).

The waveforms of the output voltage v_{pv} and output current i_{pv} of the PV emulator are shown on Fig. 4, under STC. The

load current i_{pv} tracks precisely the PV reference current i_{pvref} in steady state.

B. Step Changes in Solar Insolation

To validate dynamical performances and tracking accuracy of the proposed PV emulator, the step changes in solar insolation were induced. The simulation waveforms of the output voltage v_{pv} and the output current i_{pv} of the PV emulator, under step changes of solar insolation: 1000→600→800→400 W/m^2 (every 0.05 s), are shown on Fig. 5. The ambient temperature was constant: T=298 K.

It can be concluded from Fig. 5 that the output voltage v_{pv} and the output current i_{pv} of the PV emulator reach quickly new stationary states, for about 20 ms. As it is shown on Fig. 6, the output voltage and current have expected values in stationary states. Therefore, the dynamical response and the tracking accuracy of the proposed PV emulator are both excellent.
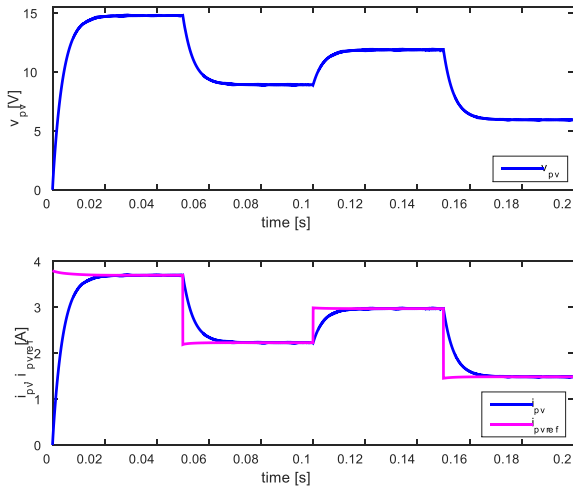

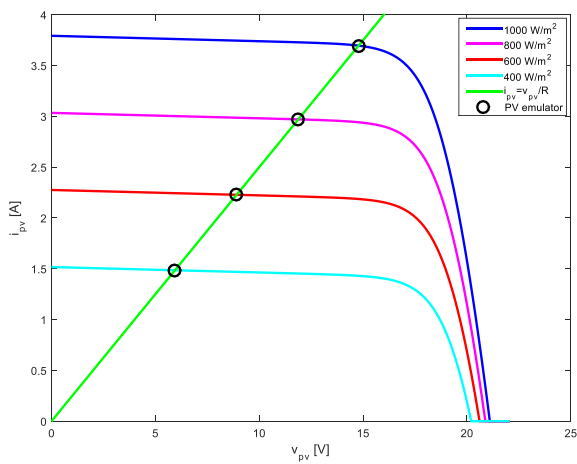Figure 5.   The output voltage and current of the PV emulator, under step changes of solar insolation: 1000→600→800→400 W/m^2 (T=298 K).

Figure 6.   Working points of the PV emulator and I-V curves of the PV model, for different solar insolations: 1000 W/m^2, 800 W/m^2, 600 W/m^2 and 400 W/m^2 (T=298 K).

C. Step Changes in Ambient Temperature

The simulation waveforms of the output voltage v_{pv} and the output current i_{pv}, under step changes of ambient temperature: 298→283→292→287 K (every 0.05 s), are given in Fig. 7. The solar insolation was constant: I_{ins}=1000 W/m^2.

The obtained working points of the PV emulator for all considered values of temperature are matched with the expected working points, as it is shown on Fig. 8.
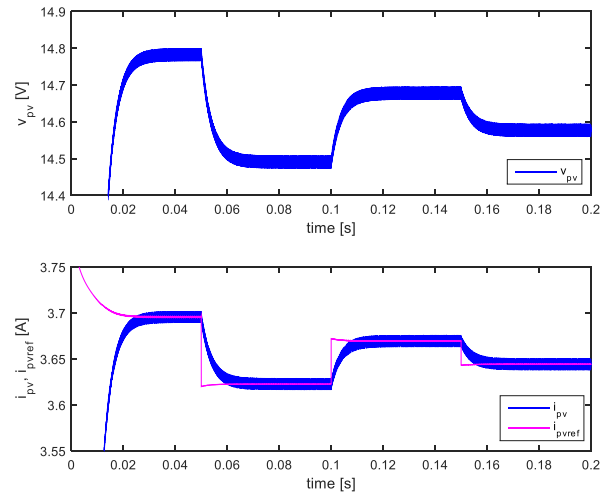

Figure 7.   The output voltage and current of the PV emulator, under step changes of temperature: 298→283→292→287 K (I_{ins}=1000 W/m^2).
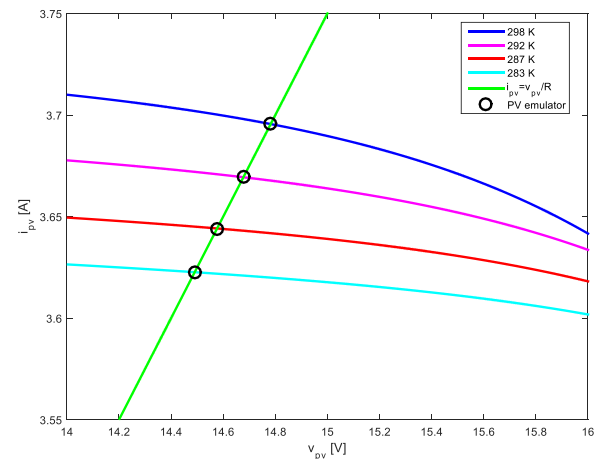

Figure 8.   Working points of the PV emulator and I-V curves of the PV model, for different temperatures: 298 K, 292 K, 287 K and 283 K (I_{ins}=1000 W/m^2).

D. Step Changes in Load

It is also very important to validate the performances of the proposed PV emulator during the changes of load. The waveforms of the output voltage v_{pv} and the output current i_{pv}, under step changes of load resistance from the value of 4 Ω to 2 Ω (t=0.05 s) and vice versa (t=0.1 s), are given in Fig. 9. The solar insolation and temperature were constant: I_{ins}=1000 W/m^2 and T=298 K.

Like in the previous cases, the transient responses finish in about 20 ms. The current i_{pv} has large over/undershoots at the beginnings of the transients. However, this is not a drawback of the control structure. Because of the step changes of load resistance, the step changes in load current normally occur.

The output voltage and current of the PV emulator have expected exact values in steady states, as it is shown on Fig. 10.
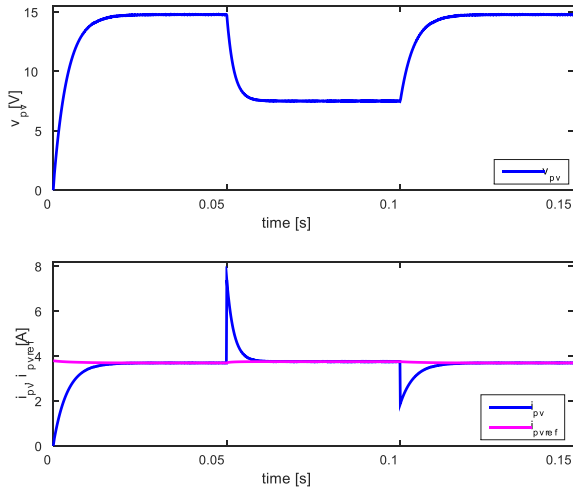
Figure 9. The output voltage and current of the PV emulator, under step changes of load resistance: 4→2→4 Ω (I_{ins}=1000 W/m², T=298 K).
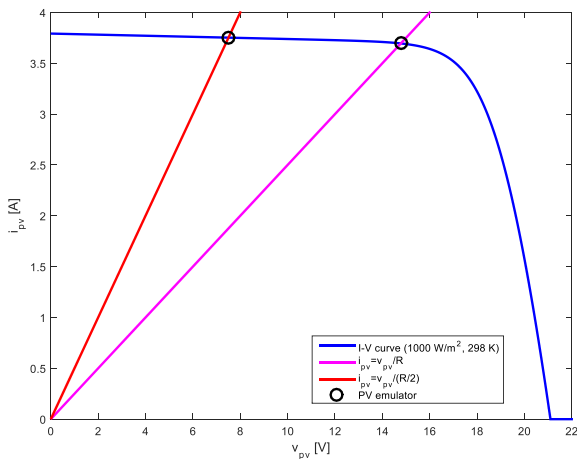

Figure 10. Working points of the PV emulator and I-V curve of the PV model, for different values of load resistance (I_{ins}=1000 W/m², T=298 K).

IV. EXPERIMENTAL RESULTS

The experimental platform of the proposed PV emulator, which is built according to Fig. 1, is shown on Fig. 11.
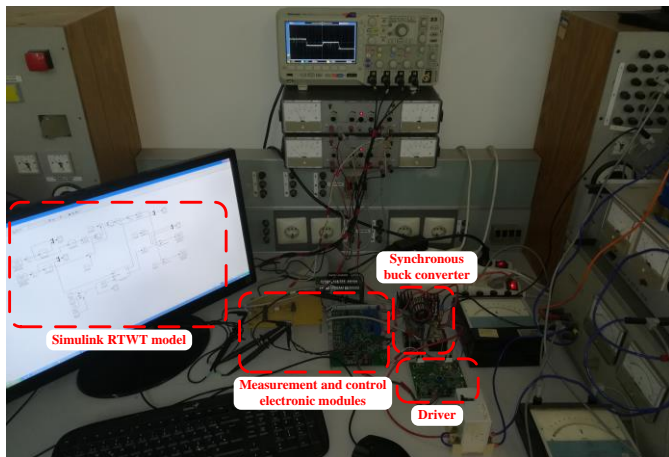

Figure 11. Experimental platform of the proposed PV emulator.

A galvanic isolated measurement of the output voltage, the output current and the inductor current of the synchronous buck converter is performed on the developed measurement

electronic module (linear optocoupler IL300 and current transducer HX 10-NP are used for galvanic isolation). The measured value of the output voltage is brought to analog-to-digital (A/D) channel (14-bit, 2 µs conversion time, ±10 V input range) of MF 624 data acquisition board, which is installed in the computer. A Simulink real time windows target (RTWT) model of the PV module acquires this measured value from the A/D channel and calculates the PV reference current, in real time. A fundamental sample time of the Simulink model is set to 25 µs. The PV reference current is exported from digital-to-analog (D/A) channel (14-bit, 10 V/µs slew rate, ±10 V output range) of MF 624 board and brought to the control electronic module. The generated control pulses for the power switches (IRF540N power MOSFETs, 100 V, 33 A) of the synchronous buck converter are fed into the driver, which has two galvanic isolated output channels.

From the above description of the experimental platform, it is evident that the galvanic isolation between the power and control stage is very important demand.

Since the maximum power of the considered PV module is about 60 W, the proposed PV emulator is designed for power ratings up to 100 W, which is enough and satisfying for education purposes.

Real time implementation of the PV model in Simulink offers many benefits: simple and user-friendly graphical design of the PV mathematical model, easy manipulation with PV module parameters, opportunity to easily set different profiles of solar insolation and temperature, visualization of the results, etc. There is no need for design of the software application of the graphical user interface, since Simulink RTWT model enables online interaction between the user and the PV emulator.

To verify the performances of the developed PV emulator, several experimental tests were conducted. The same parameters values from Table I of the proposed PV emulator, which are used in simulations, are also used in experiments.

A. Stationary States for Different Values of Insolation and Temperature

The obtained working points of the PV emulator for different values of solar insolation and ambient temperature are shown on Fig. 12.
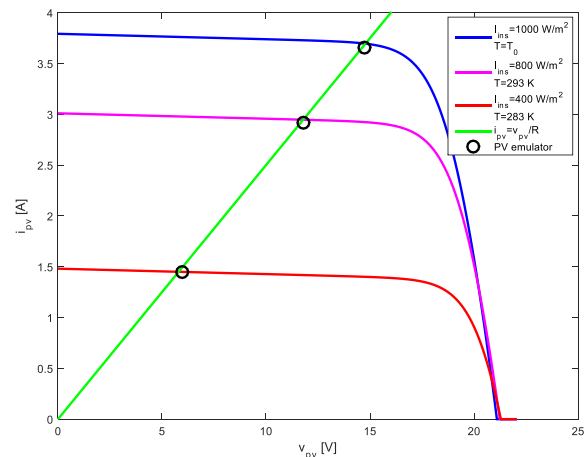

Figure 12. Working points of the PV emulator and I-V curves of the PV model, for different solar insolations and temperatures: (1000 W/m², 298 K), (800 W/m², 293 K) and (400 W/m², 283 K) – experimental results.

It is obvious from Fig. 12 that the obtained experimental values of the output voltage v_{pv} and current i_{pv} of the proposed PV emulator are almost equal to the theoretical expected values (PV voltage and current at the intersections between the I-V curves of the PV model and load working line). The steady state errors are very small (Table II).

TABLE II.   VOLTAGE AND CURRENT ERRORS IN STEADY STATE FOR DIFFERENT INSOLATIONS AND TEMPERATURES

I_{ins} [W/m²]	T [K]	Voltage error [%]	Current error [%]
1000	298	0.22	0.96
800	293	0.19	0.85
400	283	2.75	0.06

B. Step Changes in Solar Insolation

The experimental waveforms of the output voltage v_{pv} and the output current i_{pv}, under step changes of solar insolation: $1000{\rightarrow}600{\rightarrow}800{\rightarrow}400$ W/m² (every 0.1 s), are given in Fig. 13. The ambient temperature was constant: T=298 K. The waveforms are obtained with Tektronix MSO 2014 oscilloscope (100 MHz, 1 GS/s).

The experimental results from Fig. 13 are very similar to the earlier discussed simulation results from Fig. 5. Therefore, an excellent dynamical response and tracking accuracy of the proposed PV emulator are also validated experimentally.
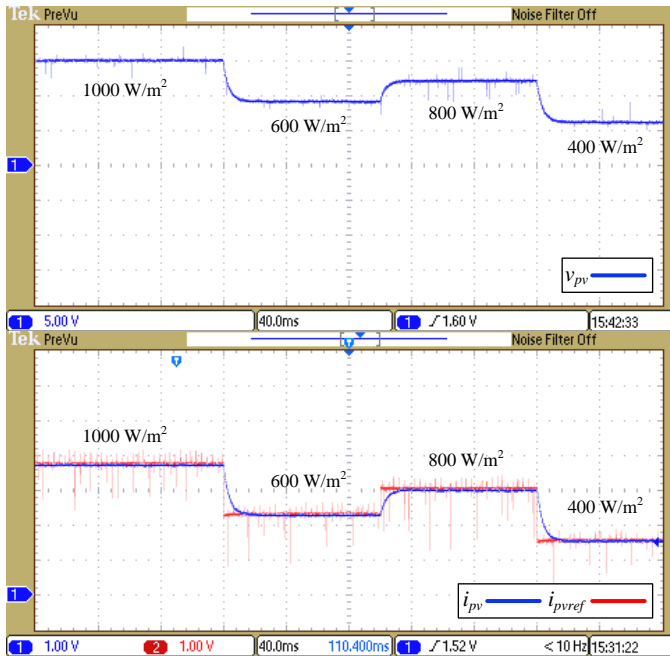

Figure 13. The output voltage and current of the PV emulator, under step changes of solar insolation: $1000{\rightarrow}600{\rightarrow}800{\rightarrow}400$ W/m² (T=298 K) – experimental results.

C. Step Changes in Load

The experimental waveforms of the output voltage v_{pv} and the output current i_{pv}, under step changes of load resistance from the value of 4 Ω to 2 Ω and vice versa, are shown on Fig. 14. The step changes of load resistance were obtained with the switch, which connects or disconnects another resistor in parallel with the load resistor R. The solar insolation and temperature were constant: I_{ins}=1000 W/m² and T=298 K.

As in the previous case, the obtained experimental results from Fig. 14 are very similar to the simulation results from Fig. 9. Therefore, a same discussion of the results can be applied here.
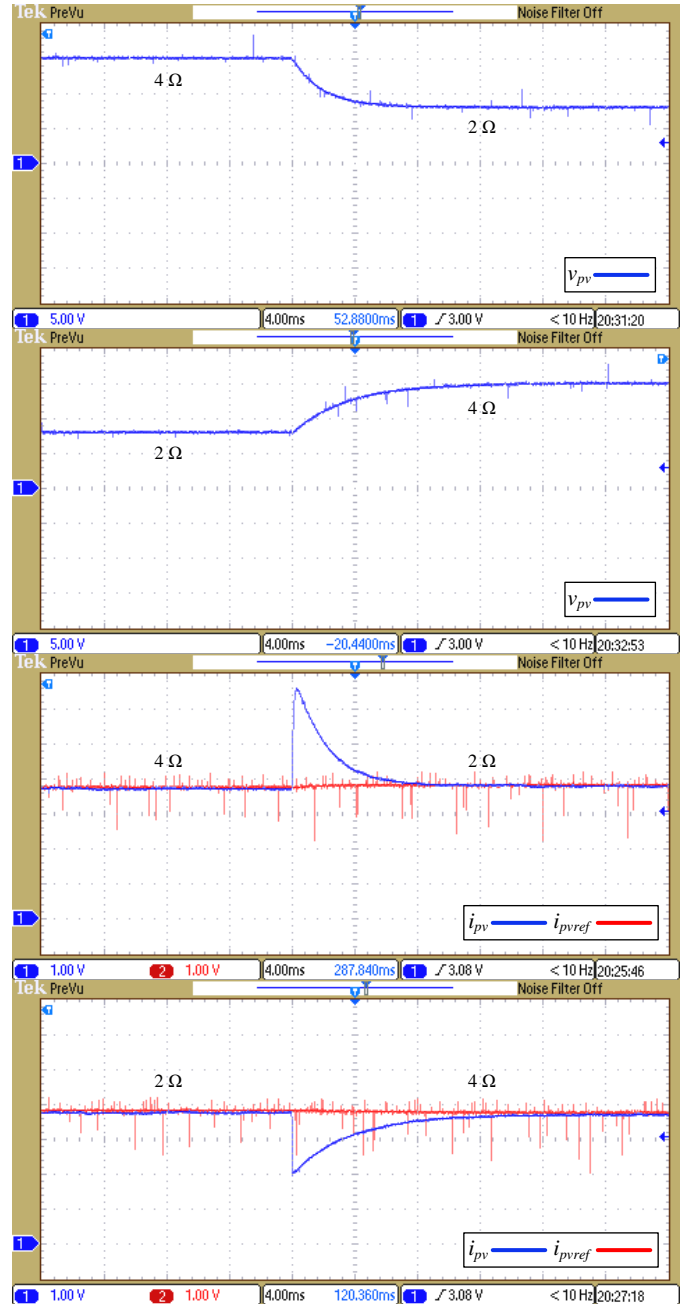

Figure 14. The output voltage and current of the PV emulator, under step changes of load resistance: $4{\rightarrow}2{\rightarrow}4$ Ω (I_{ins}=1000 W/m², T=298 K) – experimental results.

The experimental waveforms of the inductor current for both values of the load resistance are shown on Fig. 15. It is obvious that I^2 DCMC ensures equality between the PV reference current i_{pvref} (red line on Fig. 15) and the average inductor current $\langle i_L(t) \rangle_{T_s}$ (blue dashed line).

The values of the output current i_{pv} in stationary states are almost equal for R=4 Ω and R=2 Ω (Fig. 14). This is because the working points for both load resistances lie on the approximately constant-current region of the PV I-V curve (Fig. 10). To leave this region, the load resistance must be increased, for example to the value R=10 Ω. The obtained working points of the PV emulator for R=2 Ω, 4 Ω and 10 Ω are shown on Fig. 16.
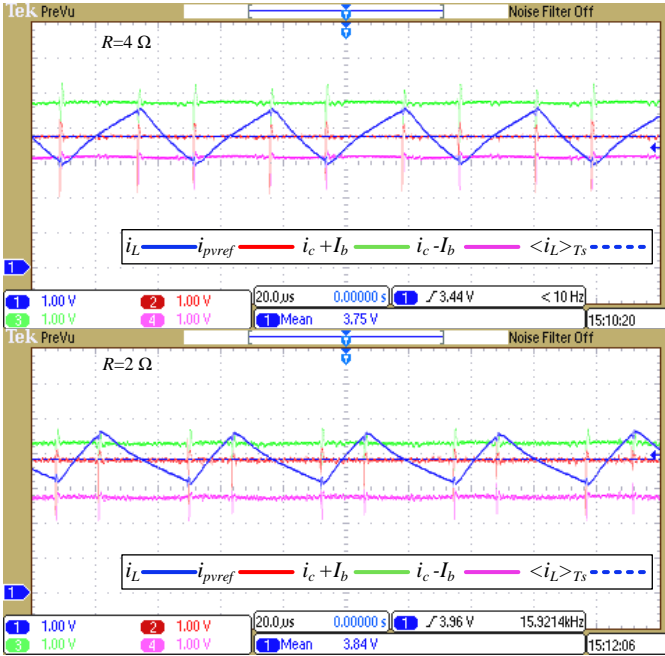
Figure 15. The experimental waveforms of the inductor current, for R=4 Ω (up) and R=2 Ω (down) (I_{ins}=1000 W/m², T=298 K).
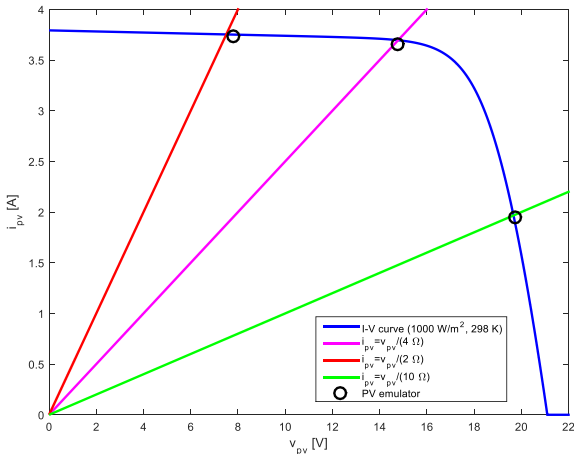

Figure 16. Working points of the PV emulator and I-V curve of the PV model, for different values of load resistance: 2 Ω, 4 Ω and 10 Ω (I_{ins}=1000 W/m², T=298 K) – experimental results.

The experimental results for step changes of the load resistance from 4 Ω to 10 Ω and vice versa, are given in Fig. 17. Obviously, the proposed PV emulator also successfully adapts to these large changes of the working points.

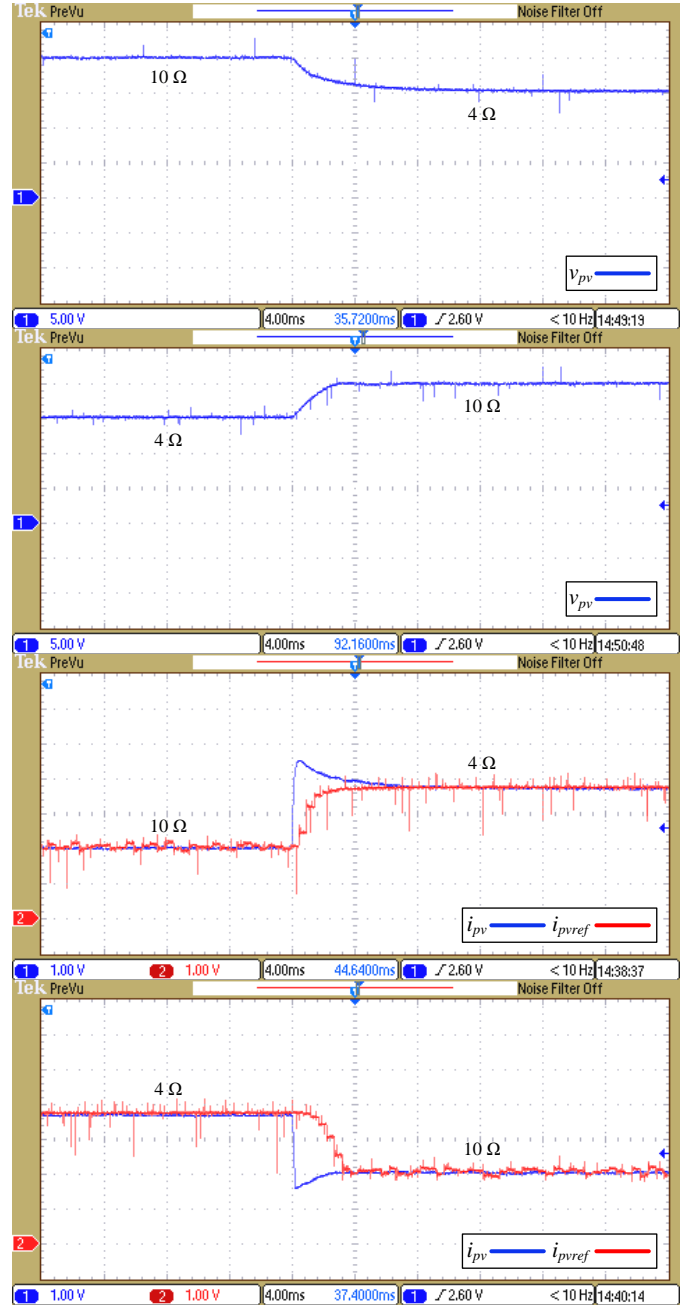Figure 17. The output voltage and current of the PV emulator, under step changes of load resistance: 10→4→10 Ω (I_{ins}=1000 W/m², T=298 K) – experimental results.

V. CONCLUSION

In this paper, the buck converter-based PV emulator with I^2 DCMC is proposed. The structure of the proposed PV emulator, its functionality and the practical realization are described in detail. Several case studies were considered in both simulations and experiments. The given simulation and experimental results confirmed excellent performances of the proposed PV emulator: fast dynamics, precise tracking of different setpoints according to the emulated weather conditions and adaptability to the emulated changes in solar insolation, ambient temperature and load. The developed experimental platform offers many benefits, which makes it applicable in education: user-friendly graphical design of the PV model in Simulink, simple manipulation with the

parameters of the PV module, possibility to easily set different profiles of insolation and temperature, online visualization of the experimental results, etc.

The existing experimental platform of the proposed PV emulator could be expanded for testing of maximum power point tracking (MPPT) algorithms, then for emulation of PV strings, where partial shading effects could be tested, etc., which are challenges for future work. The galvanic isolation between the converter and control stage allows realization of the PV emulators of higher powers. Regarding that, two solutions will be considered in future work. The first task could be development of power converter with higher voltage and current ratings, which is capable to emulate PV string. Another solution is to connect multiple proposed PV emulators into the string. In this case, each PV emulator in the string should have its own power supply at the converter's input. Also, it is possible to use only one power supply for all PV emulators in the string, however, the converters must be galvanically isolated in that case.

REFERENCES

[1] Chroma ATE Inc., "Programmable DC power supply (solar array simulation) model 62000H-S series," data-sheet.

[2] Keysight Technologies, "Photovoltaic/solar array simulation solution," data-sheet, pp. 1-12, 2018.

[3] A. Sanaullah and H. A. Khan, "Design and implementation of a low cost Solar Panel emulator," 2015 IEEE 42nd Photovoltaic Specialist Conference (PVSC), New Orleans, LA, pp. 1-5, 2015, doi: 10.1109/PVSC.2015.7356274.

[4] D. M. K. Schofield, M. P. Foster and D. A. Stone, "Low-cost solar emulator for evaluation of maximum power point tracking methods," Electronics Letters, vol. 47, no. 3, pp. 208-209, February 2011, doi: 10.1049/el.2010.2930.

[5] L. P. Sampaio and S. A. Oliveira da Silva, "Graphic computational platform integrated with an electronic emulator dedicated to photovoltaic systems teaching," IET Power Electronics, vol. 10, no. 14, pp. 1982-1992, November 2017, doi: 10.1049/iet-pel.2016.1018.

[6] F. Yusivar, M. Y. Farabi, R. Suryadiningrat, W. W. Ananduta, and Y. Syaifudin, "Buck-converter photovoltaic simulator," International Journal of Power Electronics and Drive System, vol. 1, no. 2, pp. 156-167, December 2011, doi: http://dx.doi.org/10.11591/ijpeds.v1i2.92.

[7] J. Gonzalez-Llorente, A. Rambal-Vecino, L. A. Garcia-Rodriguez, J. C. Balda, and E. I. Ortiz-Rivera, "Simple and efficient low power photovoltaic emulator for evaluation of power conditioning systems," 2016 IEEE Applied Power Electronics Conference and Exposition (APEC), Long Beach, CA, pp. 3712-3716, 2016, doi: 10.1109/APEC.2016.7468404.

[8] C.H. Balakishan and N. Sandeep, "Development of a microcontroller based pv emulator with current controlled dc-dc buck converter," vol. 4, no. 4, pp. 1049-1055, 2014.

[9] E. Koutroulis, K. Kalaitzakis, and V. Tzitzilonis, "Development of an FPGA-based system for real-time simulation of photovoltaic modules," Microelectronics Journal, vol. 40, no. 7, pp. 1094-1102, 2009, doi: 10.1016/j.mejo.2008.05.014.

[10] W. Subsingha, "Real-time photovoltaic simulator using current feedback control," Energy Procedia, vol. 89, pp. 160-169, 2016, doi: 10.1016/j.egypro.2016.05.022.

[11] W. Zhang and J. W. Kimball, "DC–DC converter based photovoltaic simulator with a double current mode controller," IEEE Transactions on Power Electronics, vol. 33, no. 7, pp. 5860-5868, July 2018, doi: 10.1109/TPEL.2017.2742461.

[12] S. M. Azharuddin, M. Vysakh, H. V. Thakur, B. Nishant, T. S. Babu, K. Muralidhar, D. Paul, B. Jacob, K. Balasubramanian, and N. Rajasekar, "A near accurate solar pv emulator using dspace controller for real-time control," Energy Procedia, vol. 61, pp. 2640-2648, 2014, doi: 10.1016/j.egypro.2014.12.266.

[13] U. K. Shinde, S. G. Kadwane, R. K. Keshri, and S. P. Gawande, "Dual mode controller-based solar photovoltaic simulator for true pv characteristics," Canadian Journal of Electrical and Computer Engineering, vol. 40, no. 3, pp. 237-245, September 2017, doi: 10.1109/CJECE.2017.2708721.

[14] H. Mekki, A. Mellit, S. A. Kalogirou, A. Messai, and G. Furlan, "FPGA‐based implementation of a real time photovoltaic module simulator," Progress in photovoltaics: research and applications, vol. 18, no. 2, pp. 115-127, January 2010, doi: 10.1002/pip.950.

[15] M. Ajaamoum, M. Kourchi, B. Bouachrine, A. Ihlal, and L. Bouhouch, "Photovoltaic panel emulators, design and implementation using rapid prototyping technique," International Review of Electrical Engineering, vol. 9, no. 5, pp. 1012-1020, 2014, doi: 10.15866/iree.v9i5.2067.

[16] S. Polo-Gallego, C. Roncero-Clemente, E. Romero-Cadaval, V. Miñambres-Marcos, and M.A. Guerrero-Martínez, "Development of a photovoltaic array emulator in a real time control environment using xpc target," In: L.M. Camarinha-Matos, S. Tomic, P. Graça (eds), "Technological innovation for the internet of things," DoCEIS 2013, IFIP Advances in Information and Communication Technology, vol. 394, pp. 325-333, 2013, Springer, Berlin, Heidelberg.

[17] S. Lale, M. Šoja, S. Lubura, and D. Mančić, "Application of I^2 technique on dual current mode control of power electronics converters," Electrical Engineering, vol. 100, no. 3, pp. 1761–1772, September 2018, doi: 10.1007/s00202-017-0653-9.

Srđan Lale was born in Sarajevo in 1987. He received B.Sc. and M.Sc. degrees at Faculty of Electrical Engineering, University of East Sarajevo, in 2010 and 2013, respectively, and PhD degree at Faculty of Electronic Engineering, University of Niš, in 2018. His research interests include power electronics, control of power electronics converters and renewable power sources. He has published over thirty scientific papers.

Milomir Šoja was born in Sarajevo in 1959. He received B.Sc. degree at Faculty of Electrical Engineering, University of Sarajevo, in 1982, M.Sc. and PhD degrees at Faculty of Electrical Engineering, University of East Sarajevo, in 2004 and 2008, respectively. His research interests include power electronics, control of power electronics converters and renewable power sources. He has published over seventy scientific papers.

Slobodan Lubura was born in Sarajevo in 1969. He received B.Sc., M.Sc. and PhD degrees at Faculty of Electrical Engineering, University of East Sarajevo, in 2000, 2006 and 2009, respectively. His research interests include mechatronics, power electronics, control of power electronics converters and renewable power sources. He has published over ninety scientific papers.

Marko Ikić was born in Sarajevo in 1986. He received B.Sc. and M.Sc. degrees at Faculty of Electrical Engineering, University of East Sarajevo, in 2009 and 2013, respectively. He is currently enrolled in PhD degree study programme Power Grids and Systems at School of Electrical Engineering, University of Belgrade. His research interests include power systems, power electronics and renewable power sources. He has published about forty scientific papers.